AN AUTOMATIC GLAUCOMA SCREENING ALGORITHM FOR NORMAL AND MYOPIA EYESIGHT USING CUP-TO-DISC RATIO AND ISNT RULE WITH SUPPORT VECTOR MACHINE

BY

WANICHA RUENGKITPINYO

A THESIS SUBMITTED IN PARTIAL FULFILLMENT OF
THE REQUIREMENTS FOR THE DEGREE OF
MASTER OF ENGINEERING (INFORMATION AND COMMUNICATION
TECHNOLOGY FOR EMBEDDED SYSTEMS)
SIRINDHORN INTERNATIONAL INSTITUTE OF TECHNOLOGY
THAMMASAT UNIVERSITY
ACADEMIC YEAR 2015

AN AUTOMATIC GLAUCOMA SCREENING ALGORITHM FOR NORMAL AND MYOPIA EYESIGHT USING CUP-TO-DISC RATIO AND ISNT RULE WITH SUPPORT VECTOR MACHINE

BY

WANICHA RUENGKITPINYO

**A THESIS SUBMITTED IN PARTIAL FULFILLMENT OF
THE REQUIREMENTS FOR THE DEGREE OF
MASTER OF ENGINEERING (INFORMATION AND COMMUNICATION
TECHNOLOGY FOR EMBEDDED SYSTEMS)
SIRINDHORN INTERNATIONAL INSTITUTE OF TECHNOLOGY
THAMMASAT UNIVERSITY
ACADEMIC YEAR 2015**

AN AUTOMATIC GLAUCOMA SCREENING ALGORITHM FOR NORMAL AND MYOPIA EYESIGHT USING CUP-TO-DISC RATIO AND ISNT RULE WITH SUPPORT VECTOR MACHINE

A Thesis Presented

By

WANICHA RUENGKITPINYO

Submitted to
Sirindhorn International Institute of Technology
Thammasat University
In partial fulfillment of the requirement for the degree of
MASTER OF ENGINEERING (INFORMATION AND COMMUNICATION
TECHNOLOGY FOR EMBEDDED SYSTEMS)

Approved as to style and content by

Advisor and
Chairperson of Thesis Committee _____
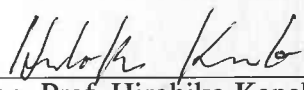Assoc. Prof. Waree Kongprawechnon, Ph.D.

Co-Advisor _____
Assoc. Prof. Toshiaki Kondo, Ph.D.

Committee Member and
Chairperson of Examination Committee _____
Pished Bunnun, Ph.D.

Committee Member _____
Assoc. Prof. Hirohiko Kaneko, Ph.D.

SEPTEMBER 2015

i

Acknowledgments

Abstract

AN AUTOMATIC GLAUCOMA SCREENING ALGORITHM FOR NORMAL AND
MYOPIA EYESIGHT USING CUP-TO-DISC RATIO AND ISNT RULE WITH
SUPPORT VECTOR MACHINE

by

Wanicha Ruengkitpinyo

Bachelor of Engineering in Electronics and Communication Engineering, Sirindhorn
International Institute of Technology Thammasat University, 2013

In this study, a new automatic glaucoma screening algorithm is proposed. Glaucoma is one of a serious eye disease which is a gateway of blindness. The main characteristic of glaucoma optic nerve head (ONH) is an expansion in size of optic cup. Many glaucoma screening systems used this characteristic as a main key to differentiate between glaucoma and non-glaucoma optic nerve. However, this can give an incorrectly classification for myopia and genetically large optic cup. Optic nerve heads of these two cases will have a larger size of optic cup than others. To overcome this limitation, two clinical indicators; cup-to-disc ratio and ISNT rule; are selected to utilize in this proposed screening algorithm. Support vector machine is also used to perform an automatic screening algorithm. Results of this study show that the proposed screening algorithm can minimize false negative cases and also improving an accuracy of a screening system. Therefore, this screening algorithm is appropriated for optic nerve heads with either normal size or large size of optic cup.

Keywords: Glaucoma, Cup-to-disc Ratio, ISNT Rule, Support Vectoe Machine, Image Processing

Table of Contents

List of Figures

List of Tables

List of Acronyms

3D   Three Dimensional

ACC   Accuracy

CDR   Cup-to-disc ratio

FN   False negative

FP   False positive

IOP   Intraocular pressure or pressure inside an eye

ISNT   Inferior, Superior, Nasal, and Temporal regions (regions of optic nerve head)

OC   Optic cup

OCT   Optical Coherence Tomography

OD   Optic disc

ONH   Optic nerve head

RGB   Red, green, and blue

ROI   Region of interests

SENS   Sensitivity

SPEC   Specificity

TN   True negative

TP   True positive

List of Notations

.	Dot product
$*$	Convolution
σ	Standard deviation
θ	Bending angle
λ	Eigenvalue
$\frac{\partial^2}{\partial x^2}$	Second-order partial derivation with respect to x
$\lvert v \rvert$	Norm of a vector
$[a\ b...]^T$	Transpose matrix
CDR_H	Cup-to-disc ratio of horizontal diameters
CDR_V	Cup-to-disc ratio of vertical diameters
DOC	Diameter of an optic cup
DOC_H	Horizontal diameter of an optic cup
DOC_V	Vertical diameter of an optic cup
DOD	Diameter of an optic disc
DOD_H	Horizontal diameter of an optic disc
DOD_V	Vertical diameter of an optic disc
ISNT	ISNT rim width
ISNT_R	ISNT ratio

Chapter 1

Introduction

Motivation and problem statements of this study are introduced in this chapter. Description of related works also included. In addition, this thesis organization and a list of our publication are also inform in this chapter.

1.1 Motivation

Glaucoma is a serious eye disease that damaged an optic nerve by increasing pressure within a eyeball. Figure 1.1 shows a different level of pressure between non-glaucoma and glaucoma eyeball. This tension can affect a vision. However, different optic nerve can handle different level of pressure. Therefore, a high level of pressure cannot damage an optic nerve that can tolerate higher level of pressure [26]. Abandon glaucoma eye as untreated can leads to permanent blindness. Presently, glaucoma is a major leading cause of blindness globally and also the first leading cause of irreversible blindness in Thailand [34].

Observing optic nerve head is useful for glaucoma diagnosis. The most famous clinical indicator for glaucoma screening algorithm is cup-to-disc ratio or CDR. Since, the expan-
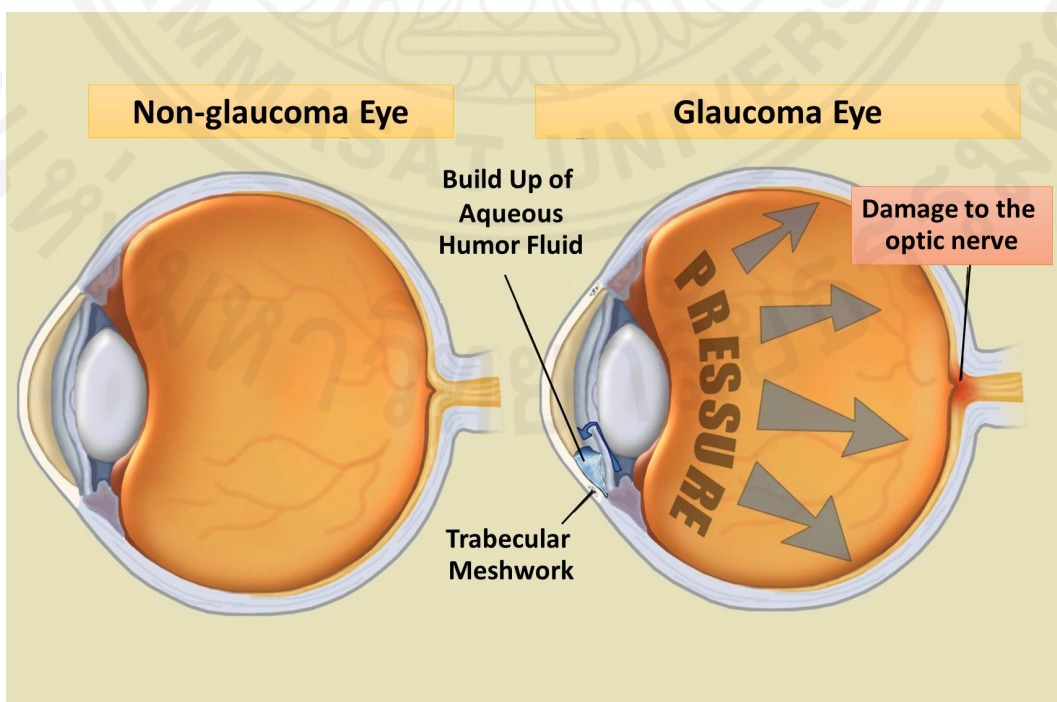
Figure 1.1: Pressure in Non-glaucoma and Glaucoma eyeball [32].
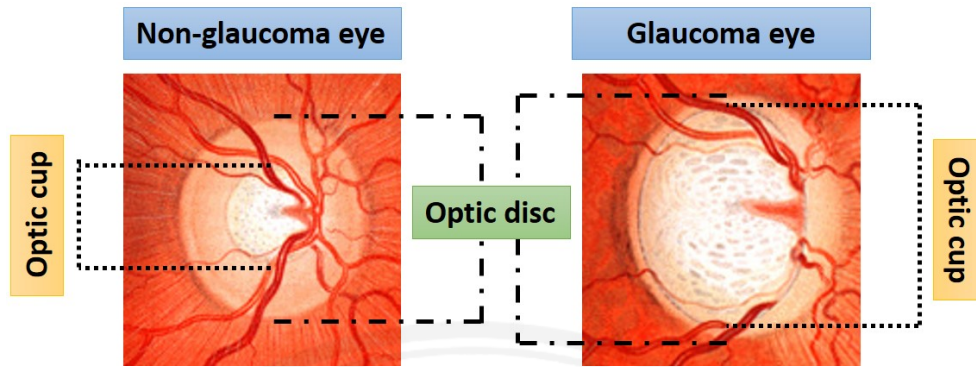
Figure 1.2: Optic nerve head of non-glaucoma and glaucoma eye [3].

sion of optic cup in optic nerve head (ONH), as shown in Figure 1.2, is a main characteristic of glaucoma. Therefore, comparing a size between optic cup and optic disc is a quick and easy method for glaucoma classification. Nevertheless, there is still some inaccurate classification. Thus, an additional indicator is needed to minimize false negative cases and also improve a accuracy of a screening algorithm.

1.2 Problem Statement

Glaucoma eyes will result in an irreversible blindness. Treatments cannot used to prevent a blindness, it just uses to slow it down. Therefore, an early diagnosis is important for eye health of patients. However, this can only be done by an expertise ophthalmologists. Special camera and equipment are also needed for the diagnosis and only experts can use these equipment. Both expertise ophthalmologists and special equipment for glaucoma diagnosis can only be found at large government hospitals and private hospitals in large cities, such as Bangkok and Chaing-mai, because of their expensive expenses. This will result in a late diagnosis for non-wealthy patients. Automatic glaucoma screening algorithm can be used for overcome these limitations.

Many glaucoma screening algorithms have been developed. Cup-to-disc ratio (CDR) is the most famous clinical indicator for many screening algorithms. CDR is used to compare a size between an optic cup and an optic disc. An eye with a large value of CDR is possibly to have a glaucoma. As a consequence of using only CDR as an indicator, there are two special cases that usually have a false classification [22]which are myopia eyes and genetically large optic cup eyes. These cases will have a larger optic cup than others. A comparison of non-glaucoma ONH between normal-eyesight and myopia (near-eyesight) is demonstrated in

2
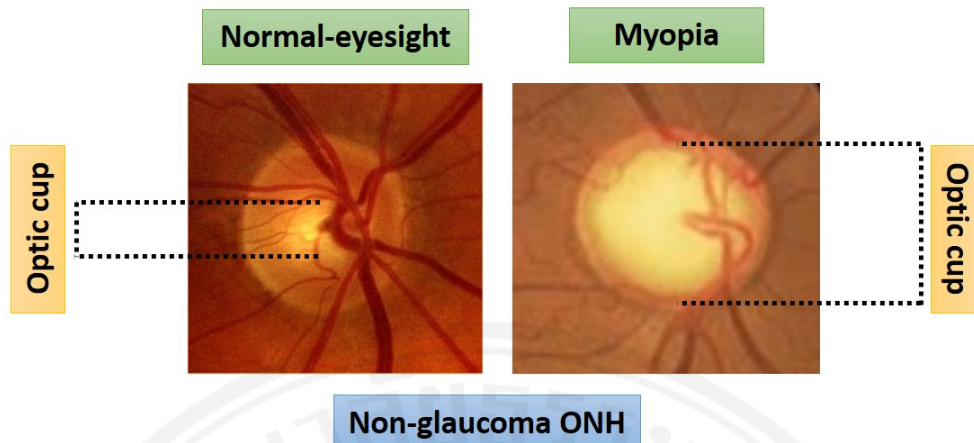
Figure 1.3: Non-glaucoma ONH of normal-eyesight and myopia (near-eyesight) [35] [22].

Figure 1.3. To conquer this limitation, others clinical indicators that do not interest in a size of optic cup should be co-operated with CDR in the screening algorithm.

1.3 Related Works

There are numerous researches about screening glaucoma that can be used by untrained ophthalmologists. These researches show that screening glaucoma with less expense can give a high efficiency result [4], [5], [7], [18], [19], [27], [37]. In these researches, image processing based on clinical indicators of glaucoma classification is performed to reduce costs from expensive equipment such as Optical coherence tomography (OCT) camera and Scanning laser polarimetry. All of them is using retinal image from a Fundus camera, Figure 1.4, which is cheapness compares to OCT camera and this camera can mostly find in every hospital. The authors will call images from Fundus camera as fundus images. Most of screening systems from these researches are using only one clinical indicator [4], [7], [18], [19], [27], [37]. However, the most famous clinical indicator is cup-to-disc ratio (CDR) [4], [5], [27], [37]. Hence, this study is also used CDR for glaucoma classification.

There are many characteristics for a glaucoma optic nerve head (ONH). Each clinical indicator is focusing in different characteristic. The interested characteristic of CDR is a size of optic cup comparing to a size of optic disc. Optic cup and optic disc area can be found by using image segmentation and 3D image. Fundus images are processed by image segmentation to locate optic cup and optic disc in C. Burana-Anusorn et al.[4], P. Vejjanugraha et al.[27], and W. Ruengkitpinyo et al.[37]. While in Chih-Yin Ho et al.[5], fundus images are processed to become 3D images which use to locate optic cup and optic disc. Even though

3
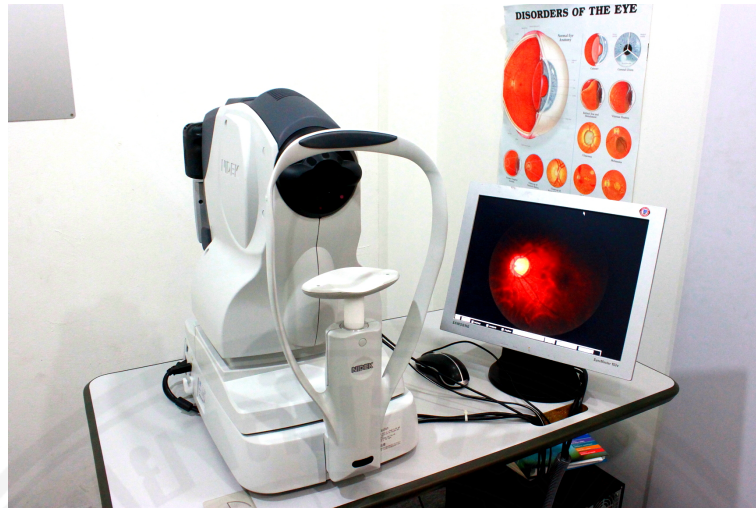
Figure 1.4: Fundus camera [13].

both methods can be used to locate both optic cup and optic disc, image processing is using much less computational time. In consequence, image segmentation technique is selected to be used in this study. By using only CDR in a screening system may not suitable for some cases. Myopia and genetically large optic cup retinal are the cases that using only CDR may cause a false classification because they have a larger optic cup than others. Therefore, an additional indicator besides CDR is needed to classification these two cases. As Murray Fingeret mentioned in his article [22], ISNT rule can be used to indicate glaucoma for large optic cup cases. This indicator is considering a width of neuroretinal rim, not a size of optic cup. This makes a rim width based on ISNT become an appropriated additional indicator for the screening system.

The area between a optic cup and a optic disc is called rim width. Rim width based on ISNT rule is a rule that helps to identify glaucoma by observing rim widths in each region of an optic nerve head [24]. Before observing rim widths, optic nerve head should be divided into four regions; inferior (I), superior(S), nasal (N), and temporal (T). Darsana S. et al. [8] proposed mask image generation for segmenting retinal fundus image into ISNT quadrants using centroid method. Then optic cup boundary should be located. Apart from using image segmentation, retinal vessels can also use to indicates optic cup boundary. This technique is appear in W. W. K. Damon et al. [38]. Retinal vessels are different in size, hence, multi-scale vessel enhancement filter is suitable for retinal vessels. Hessian based filter proposed by A. F. Frangi et al. [2] is very famous for detected retinal vessels. Rim width can be measured and observe after the above steps are done according to M. H. Tan et al. [20].

The purposed of this study is to develop an automatic glaucoma screening system that can be used by a non-expertise. K. Chan et. al. [16] and T. Yu et. al [14] are used machine learning to create an automatic classifier. There are many kinds of machine learning. Choosing a suitable machine learning for the system is also a key point. The chosen machine learning should base on a type of input and output data. For this study, a binary classifier called support vector machine is selected.

1.4   Thesis Organization

The thesis is organized as follows. Background of this study is described in Chapter 2 while methodology is introduced in Chapter 3. Chapter 4 is a results and analysis section. The last chapter in this thesis is Chapter 5 which is a conclusion of this study.

1.5   Publication

This study results in the following publication:

- W. Ruengkitpinyo, W. Kongprawechnon, T. Kondo, P. Bunnun , and H. Kaneko, "Glaucoma Screening using Rim Width based on ISNT Rule", Proceedings of the 6th International Conference on Information and Communication Technology for Embedded Systems (ICICTES), 2015

- W. Ruengkitpinyo, P. Vejjanugraha, W. Kongprawechnon, T. Kondo, P. Bunnun , and H. Kaneko, "An Automatic Glaucoma Screening Algorithm using Cup-to-disc ratio and ISNT rule with Support Vector Machine", Proceedings of the 41st Annual Conference of the IEEE Industrial Electronics Society (IECON), 2015

Chapter 2

Background

This chapter gives the background knowledge of this thesis. An explanation about eye anatomy and glaucoma are the first two sections for this chapter. Clinical indicators for glaucoma analysis are described in the last section, especially, cup-to-disc ratio (CDR) and ISNT rule which is utilized in this study.

2.1 Eye Anatomy

The purpose of this study is to develop an automatic screening algorithm for glaucoma. Therefore, understanding an eye anatomy is an advantage for developing the algorithm. The human eye is composed of many different parts as displayed in Figure 2.1. They are all working together to act as a camera for human body. Many symptoms can be used as warning signs for glaucoma. Nausea and vomitting accompany with the severe eye pain, watery eyes or excess tearing, and Halos aroung lights are example symptoms [21]. Meeting ophthalmologists is recommended for examine an eye health. Some changes which are characteristics of glaucoma could be detected. For example, watery eyes might caused by aqueous humor cannot drain because the drainage system of an eye is clogged [12]. However, the selected glaucoma characteristics for this study is occurred within an optic disc.

The optic nerve head (ONH) or the optic disc (OD) is where the optic nerve connects to the retina. Major blood vessels that supply retina also enter the eye at ONH. According to Figure 2.2, optic nerve head or optic disc is the bright area. While, the brightest area that usually locates near the center of optic disc is optic cup (OC). The area between boundaries of optic cup and optic disc is called neuroretinal rim width.

The symptoms of glaucoma that happen in this area are enlargement of optic cup and the compression of neuroretinal rim width. To observe these symptoms, boundaries of optic cup and optic disc have to be located. The boundary of optic disc can be easily located by contrasting light intensity between optic disc area and its neighbor areas. However, detecting the boundary of optic cup is ambitious. Using the same techniques as locating the optic disc is inadequate. New technique should be applied. As mention before, major retinal vessels are entered retina at optic disc. To be more specific, they infiltrate at optic cup boundary [38]

6
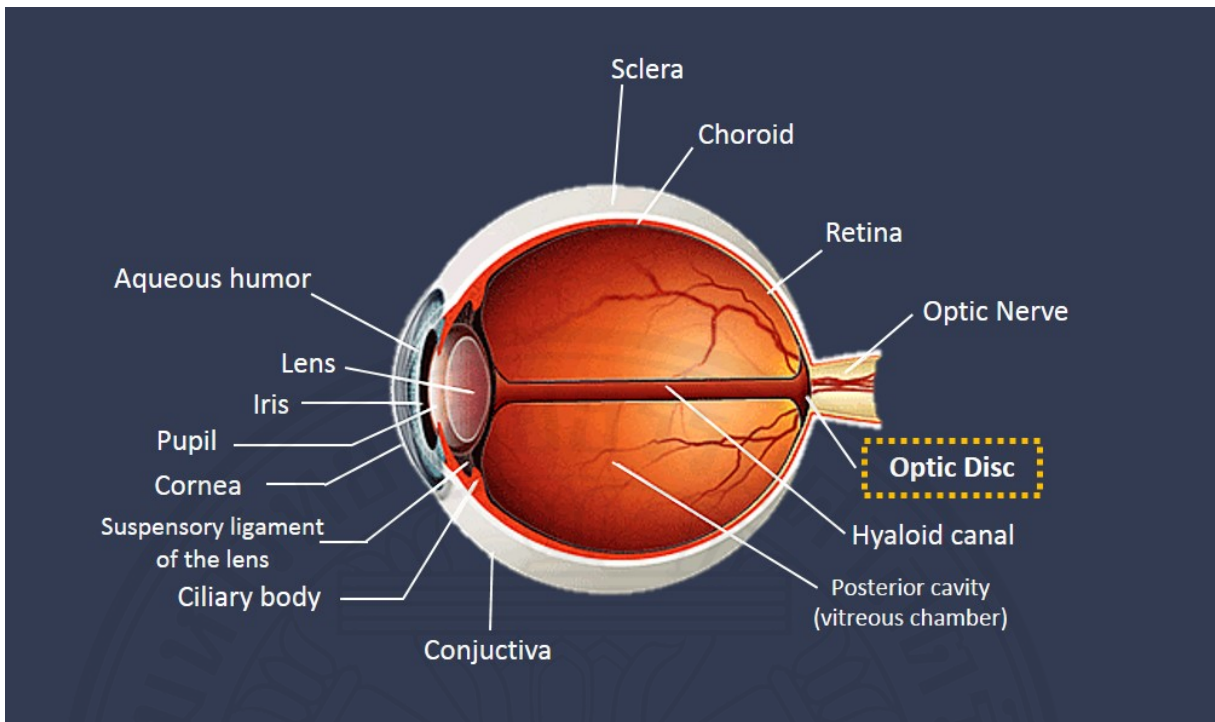
Figure 2.1: Eye Anatomy [40].
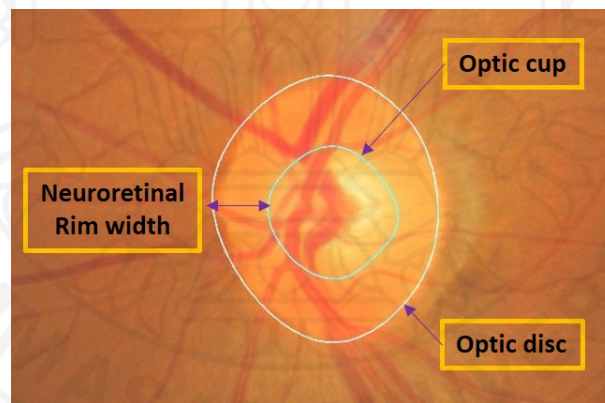
Figure 2.2: The appearance of optic nerve head (ONH)

as shown in Figure 2.3. This can be seen as bending vessels and this eye anatomy can be used to estimate the optic cup boundary [38]. The prove of the bending vessels is presented in Figure 2.4.

Besides from using retinal vessels to detect optic cup, it can use to determine the side of an eye. The optic nerve head can be segment into four regions as in Figure 2.5. I, S, N and T are abbreviation of inferior, superior, nasal and temporal which are four region of the eye. Inferior is the bottommost region where uppermost region is superior region. Nasal means nose, therefore nasal region is located near the nose. The last region is temporal. Its location is contrary to nasal region. According to Figure 2.5, nasal region of left and right eye are
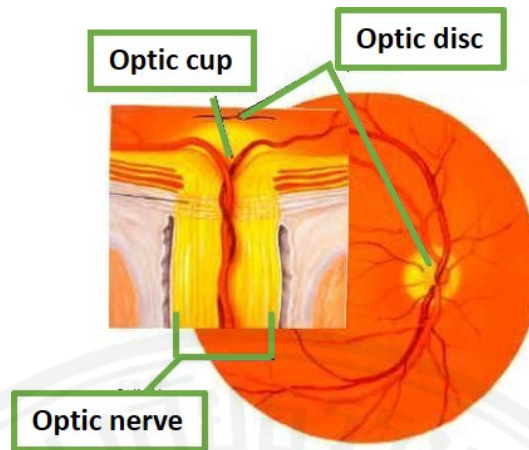
Figure 2.3: Retinal vessles enter at the optic cup boundary [15]
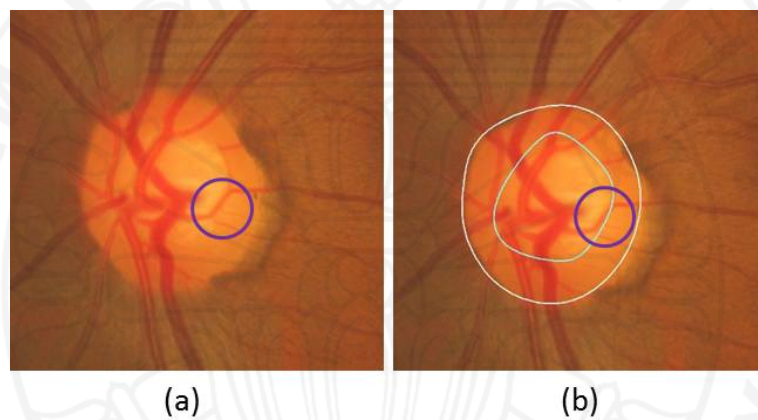
Figure 2.4: Optic cup boundary estimation by using vessel bending
(a) Fundus image (b) Fundus image with hand-drawing by ophthalmologists

placed in different area. Retinal vessels are also entering retina at nasal region. As a result, a side of the eye can be determined by inspect retinal vessels. In a case that more retinal vessels appear in the left side of a fundus image than the right side, that eye is a left eye. On the contrary, a right eye will have more retinal vessels in the right side of a fundus image. Figure 2.6 demonstrates fundus images of a left eye and a right eye.

2.2 Glaucoma

Eye is an important organ that helps us to see things. Using eyes in improperly ways can damage an eye health. Currently is a smart phones era, everyone is staring on their screens all day. These can leads to unhealthy eyes. Especially who has an myopia eye or near-sight eye, glaucoma can develop as a result from staring on the screens for a long time [25].

Glaucoma is a serious eye disease which usually occurs with seniors. In Thailand, major-
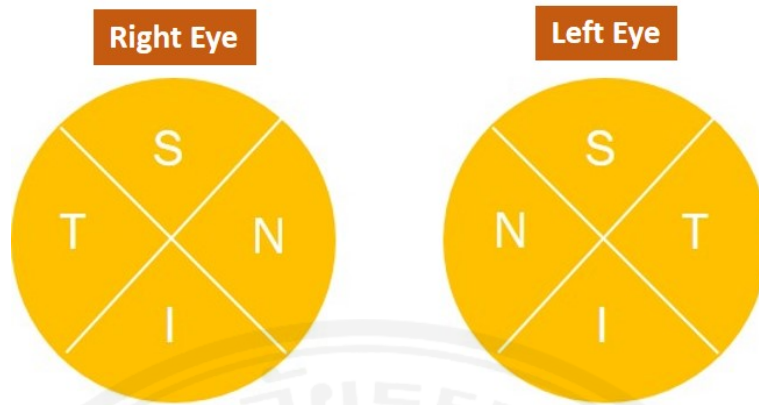
Figure 2.5: Four regions of the eye
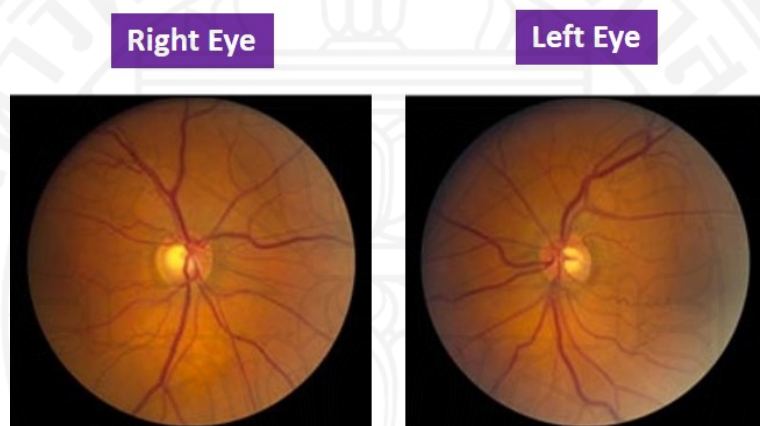
Figure 2.6: Fundus images of a left eye and a right eye

ity of seniors with an age over 60 year olds has glaucoma. Abnormal optic nerve is a result from glaucoma. There are many risk factors for glaucoma development. Heredity is one of a risk factor of glaucoma as same as diabetes. If your direct relatives have glaucoma, there is a high chance for you to have glaucoma when you are getting older. Having diabetes, using medicine that has steroids and an eye infections are other risk factors for glaucoma development.

Glaucoma can divide into several types. Open-angle and angle-closer are two main types of glaucoma. These are marked by increase of intraocular pressure (IOP) or pressure inside the eye [11]. Open-angle glaucoma is the most common type of glaucoma which caused by the slow clogging of drainage canals, results in gently increase intraocular pressure. While angle-closure glaucoma is rarely found and caused by blocked drainage canals which results in a sudden rise in intraocular pressure. Open-angle closure glaucoma is interested in this study.

Glaucoma is a cause of vision loss and this loss is irreversible. Thus, early detection

is important for glaucoma. Many indicators are used to identify glaucoma status. These indicators will thoroughly explain in the next section. After glaucoma status is identified, treatments will begin. Preventing vision loss is an objective of glaucoma treatment. Eye drops, pills, laser surgery, conventional surgery and, a combination of these methods are used to treat glaucoma [36]. Eye drops is used for primary treatment. It is used to control intraocular pressure. Supposing that eye drops is not sufficient to control the pressure, pills will be used as an additional treatment. Surgical procedures will take place only when medications do not accomplish the desired results or have unbearable side effects. Laser surgery becomes popular because of less surgery time and painless. Patients can go home after the laser surgery was completed. After trying eye drops, pills and, laser surgery but intraocular pressure still high, ophthalmologists may suggest conventional surgery. After this surgery, fifty percent of patients are no longer required glaucoma medications. Forty percent of who still need the medication has a better control of their intraocular pressure.

2.3 Clinical Indicators

Early glaucoma detection is an advantage for patients. In clinical, many indicators can be used to evaluate ONH for detecting glaucoma. This study is interested in open-angle glaucoma, as mentioned in previous section. Patients with open-angle glaucoma usually present with three exam findings [33]. The first examine is elevated eye pressure. The eye pressure is measured by using a Goldman applanation tonometer or a Tonopen. The second examine is repeatable visual field loss. Observing changes in ONH is the last examine. This can be done by monitoring fundus images. Cup-to-disc ratio and rim width based on ISNT rule which is our interested indicators are two of the indicators for this last examine.

2.3.1 Cup-to-disc Ratio

There are several changes in glaucoma ONH. Expanding optic cup is one of the changes. Cup-to-disc ratio (CDR) is a clinical indicator that uses to inspect this modification. Optic cup diameter divided by optic disc diameter is a CDR calculation. The more CDR value is closer to 1, the more damage the ONH has. CDR can be calculated in both horizontal and vertical direction. However, vertical CDR is more popular for clinical analysis. Optic cup expands in vertical direction before horizontal direction is a reason [29]. This can be clearly

seen in Figure 2.7. There is no specific value of CDR to indicate glaucoma but the range to classify glaucoma and non-glaucoma is around 0.5 to 0.7. The assort value is depends on each ophthalmologist. For this study, both vertical and horizontal CDR with a value of 0.65 is selected to use for a clinical classification. Nevertheless, an inaccurate classification still exits when CDR is utilized with myopia or genetically large optic cup cases. Since, these cases are having larger optic cup size than others.
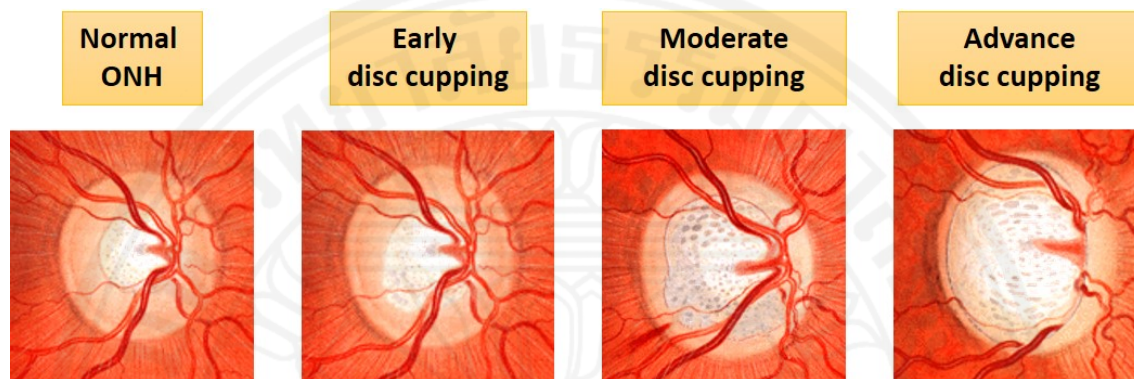
Figure 2.7: State of optic cup expansion [3]

2.3.2 ISNT rule

By attentively monitoring fundus images, optic cups can be notice that it is located slightly off-center of optic discs. As a result, neuroretinal rims width in each eye section are uneven [33]. This is a beginning of ISNT rule. Monitoring neuroretinal rim width in each ONH sections is an objective of this indicator. Therefore, this rule is named after four regions of ONH; Inferior, Superior, Nasal and Temporal. Besides from being a name of the regions, neuroretinal rim width of non-glaucoma ONH should order as same as its name (ISNT). The thickest neuroretinal rim width should be an inferior rim width. The second and the third thickest are superior rim width and nasal rim width, respectively. Temporal rim width is the thinnest. An ONH with different orders of neuroretinal rim width apart from this order, (I>S>N>T), should be suspect as a glaucoma ONH. Neuroretinal rim width of non-glauocma ONH and glaucoma ONH are compared in Figure 2.8.
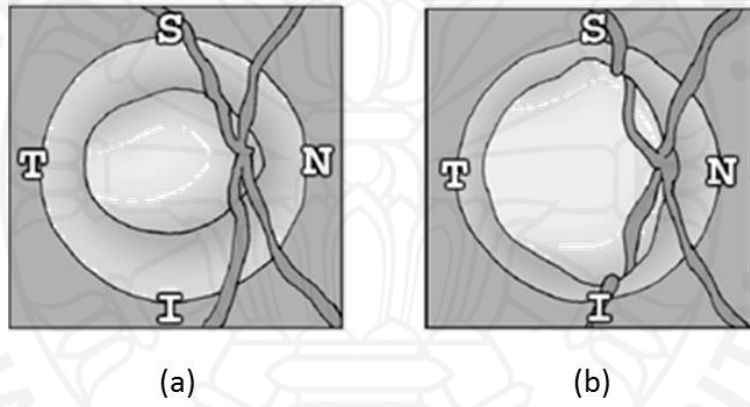
Figure 2.8: Comparison between non-glaucoma and glaucoma ONH in a term of
neuroretinal rim width [33]
(a) Non-glaucoma (b) Glaucoma

Chapter 3

Methodology

A methodology of this study is explained in this chapter. All three steps; pre-processing, retial analysis, and automatic classification; will be described. Figure 3.1 shows a framework of proposed screening system.
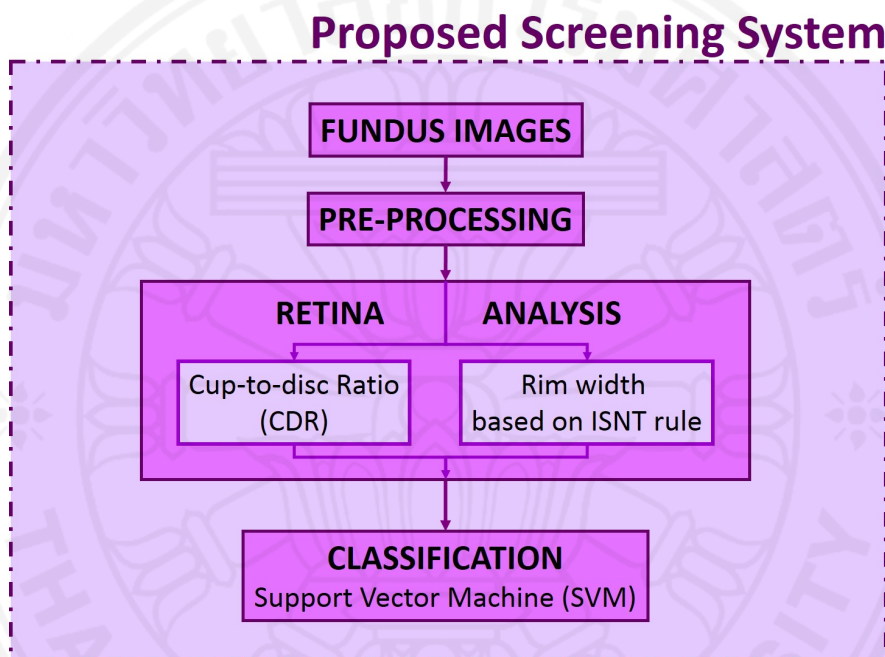
Figure 3.1: Framework of proposed screening system

3.1 Pre-processing

This is the first step of the purposed screening system. Input images for the system are prepared within this step. Fundus images which are used as initial images and a process to select region of interest (ROI) are explained in this section.

3.1.1 Fundus Image

Fundus images are captured by a fundus camera. Interior surface of an eye is shown in fundus image, covering the retina, optic disc, macula, and posterior pole. Ophthalmologists and trained medical professionals are analyzed fundus images for monitoring progression of a disease that has retinal changes as its symptoms, including glaucoma. Comparing to

ophthalmoscopy, that can be used to observe an inner surface of an eye for eye examination, fundus image needs larger equipment. However, an advantage over ophthalmoscopy is retinas can be captured to be examined by specialists at anywhere and anytime. Moreover, fundus images are less expensive than OCT images which are 3D retinal images captured by OCT camera.

One of the objectives of this study is to develop an automatic screening system that can be used in every hospital by untrained ophthalmologists with low cost. Therefore, retinal images from fundus camera or fundus images are satisfied the needs. Fundus images can be found in most of the hospital and do not have high costs. Also, it has been used as initial images for many glaucoma screening system [4], [5], [7], [18], [27], [37].

In this study, all fundus images and its state of glaucoma are obtained from Autofocus Fundus Camera (NIDEK AFC-230), Mettapracharak Hospital, Nakornpathom, Thailand. The total of 113 fundus images is used as a data set for the proposed system. These images can be classified by using two different basis information, glaucoma status and eyesight. By using glaucoma status, 54 glaucoma eyes with 59 non-glaucoma eyes are the combination of this data set. Also, this data set can be classified as 15 myopia (near-eyesight) eyes and 98 normal-eyesight eyes by using eyesight as a basis information.

3.1.2 Region of Interested Image (ROI)

All inner surface of an retina can be captured and displayed in one fundus image. Besides from using an entire image, using only the optic nerve head (ONH) area is sufficient for this screening glaucoma system. Thus, cropping fundus images to have only the region of interested is appropriated. Less computational time for screening algorithm is an advantage of this step.

The region of interests of this study is the optic nerve head (ONH). Accordingly, ONH localization is the main step of the process. ONH region is noticed as a brighter pallor or higher color intensity than the surrounding retinal area. Therefore, knowing the maximum intensity of a fundus image can leads to ONH localization. Intensity-weighted centroid technique is applied to find the bright area or ONH area in the first step [39]. Next, the centroid of ONH is found for being an reference point for cropping the fundus image. Then, the image is cropped and remains only the region of interest area and its neighbor pixels.

For this study, all fundus images are obtained from Mettapracharak hospital. Its original

size is 2912 x 3166 pixels. After cropping and remains only the region of interest (ROI), 500 x 500 pixels is its new size. This cropped images are called ROI images. The steps for creating ROI images are demonstrated in Figure 3.2. These ROI images are used as initial images for the proximate step, retina analysis.
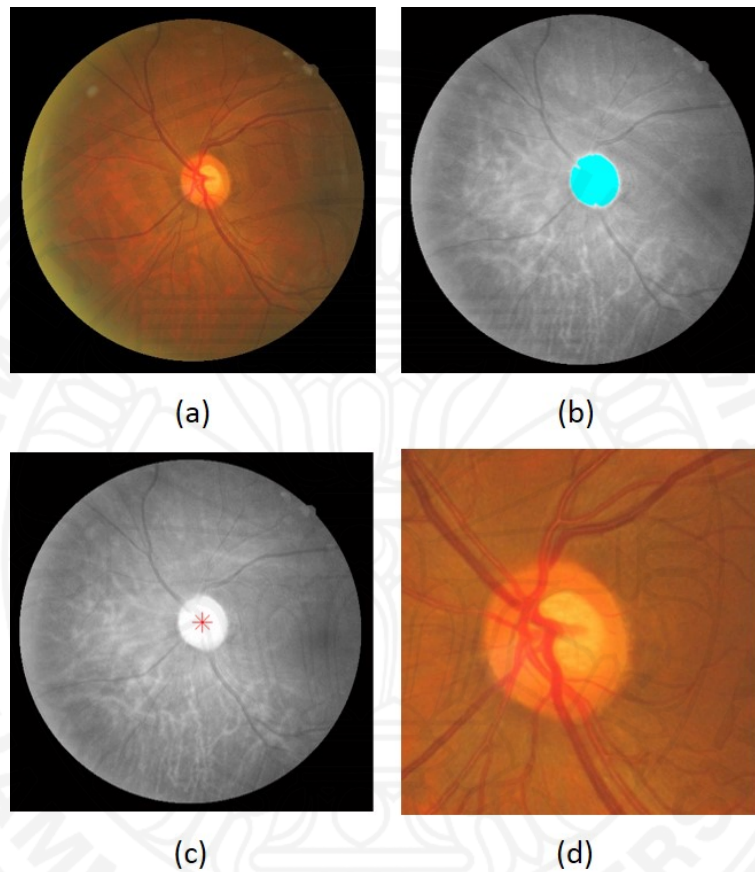
Figure 3.2: Retinal image
(a) Fundus image (b) Brightest intensity area (blue area)
(c) Centroid of ONH (red spot) (d) ROI image

3.2 Retina Analysis

After getting ROI images, retina analysis step can be proceed. In this step, all ROI images are analyzed by image processing techniques based on clinical indicators for glaucoma evaluation. Two clinical indicators that have been used for this screening algorithm are cup-to-disc ratio (CDR) and rim width based on ISNT rule. Analyzing images based on these two indicator are processed in parallel.

3.2.1 Cup-to-disc Ratio

Cup-to-disc ratio is an indicator that concern about the size of an optic cup comparing to the size of an optic disc. CDR can be calculate by using Equation 3.1. Hence, both optic cup (OC) and optic disc (OD) should be segmented. The framework of cup-to-disc ratio is shown in Figure 3.3.

$$CDR = \frac{DOC}{DOD} \tag{3.1}$$

where *CDR*   : is cup-to-disc ratio.

     DOC   : is a diameter of an optic cup.

     DOD   : is a diameter of an optic disc.
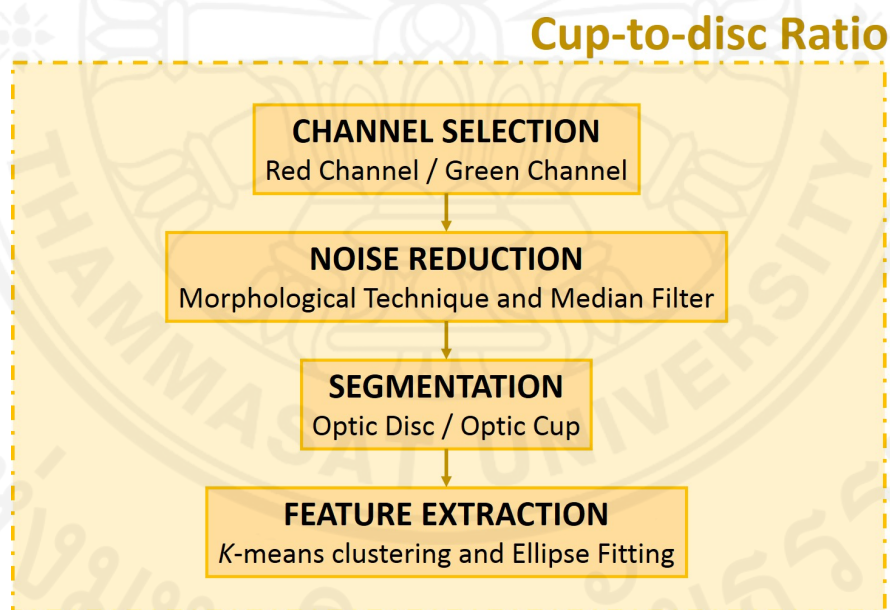
Figure 3.3: Framework of cup-to-disc ratio

Channel Selection

For the segmentation, ROI images from a previous step are used as input images. ROI images are color images (RGB images) that can be split into 3 color channels; red, green, and blue channel. After images are read in these three channels, grayscale images are generated. Red items are much brighter in red channel. In the same way, green and blue objects are much

16

brighter in green and blue channel, respectively. Suitable color channel for optic cup and optic disc segmentation should be choose. According to Figure 3.4, red channel is suited for optic disc segmentation while green channel is appropriated for optic cup segmentation. Henceforth, output images from red channel and green channel are called R images and G images.
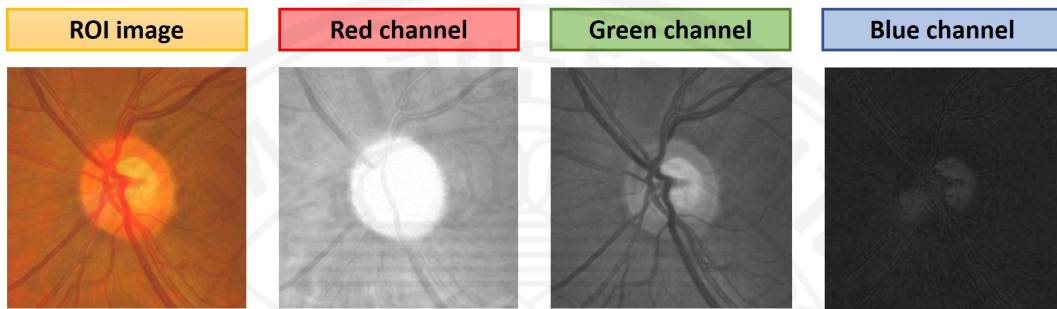
Figure 3.4: Reading ONH in different channels

Noise Reduction

After reading ROI images in color channels, some noises still exist. In this case, retinal vessels are noises of the segmentation [31]. To remove vessels, morphological technique and median filter are applied to the R and G images [27], [37].

Morphological technique is one of an image processing technique that relate to the shape of an image [23]. Only relative ordering pixel values is its interest, not their intensity values. Fundamental operations of morphological technique are erosion and dilation. Erosion can compress the size of an image by stripping away both outer and inner boundaries pixels of the image. In contrast, dilation is used to enlarge the image by adding pixels at outer and inner boundaries of the image. Opening and closing are compound operations of morphological technique. Performing erosion follows by dilation is an opening technique which use to open up a gap between objects. Closing technique is used to fill holes or making a closed area as same as its name by performing dilation before erosion. In R and G images, hole pixels are dark pixels, which is retinal vessels. Therefore, closing operation is utilized to remove vessels in this algorithm. Then, median filter is executed to smoothen the images by using the median value of neighborhood pixels [10].

Segmentation

The next step is optic cup and optic disc segmentation. However, appearance of optic cup and optic disc is not clearly seen. To overcome this problem, power law transformation is applied. Power law transformation is an image processing technique that use for improving brightness of images [30]. Equation 3.2 is an equation of power law transformation. When the gamma is between zero and one, images become brighter. Conversely, images become darker when gamma is greater than one. For this study, gamma is set equal to five.

$$S = Cr^{\gamma} \tag{3.2}$$

where S : is an output value.

     r : is an input value.

     C : is a constant value.

     γ : is a gamma compression when $0 < \gamma < 1$.

         : is a gamma expansion when $\gamma > 1$.

Canny edge detection is applied afterwards to detect optic cup and optic disc boundaries. It is a Gaussian edge detection, its performance is based on a Gaussian value [28]. Gaussian filter with standard deviation of 1.4 is used in this study. The distinctive point of canny edge detection from others is it has two threshold values which can help to suppress noises. Nonetheless, some noise may stills exist.

Features Extraction

To get rid of the noises, selecting potential candidates for optic cup and optic disc boundaries can be done by using *k*-means clustering. *K*-means clustering is a clustering algorithm that uses inherent distance information of each input points to classify the points into multiple classes [1]. However, optic cup and optic disc are not perfectly circular objects. Thus, ellipse fitting is applied to smooth the selected boundaries [4]. Equation 3.3 is a conic equation of the ellipse that use to find distance of the point (x,y) to the conic $F(a,x) = 0$. This conic equation can detect ellipse in any orientation, which means detecting ellipsoids with other orientation rather than $0°$ or $90°$ is possible. Ellipses fitting is usually based on least square

fitting algorithm as display in Equation 3.4. Assuming the curve that minimizes the algebraic distance ($F(x, y)$) over the set of N data points in the least square sense as the best-fit curve.

$$F(a, x) = a \cdot x = ax^2 + bxy + cy^2 + dx + ey + f = 0 \qquad (3.3)$$

where $F(a, x)$: is an algebraic distance of point (x, y) to the conic $F(a, x) = 0$.

      a : is $[a \quad b \quad c \quad d \quad e \quad f]^T$, constant values of an ellipse.

      x : is $[x^2 \quad xy \quad y^2 \quad x \quad y \quad 1]^T$, values of point (x,y).

$$\sum_{i=1}^{N} F(x_i)^2 \qquad (3.4)$$

where N : is an amount of points in the data set.

Measuring diameters of optic cup and optic disc in both horizontal (DOC_ H and DOD_ H) and vertical directions (DOC_ V and DOD_ V) are done later, following by CDR calculation for both vertical (CDR_ V) and horizontal (CDR_ H) directions as the last step. Values of CDR and the diameters, as shown in Figure 3.5, are utilized as features in the classification step. All steps of retina analysis based on CDR indicator are displayed in Figure 3.6.
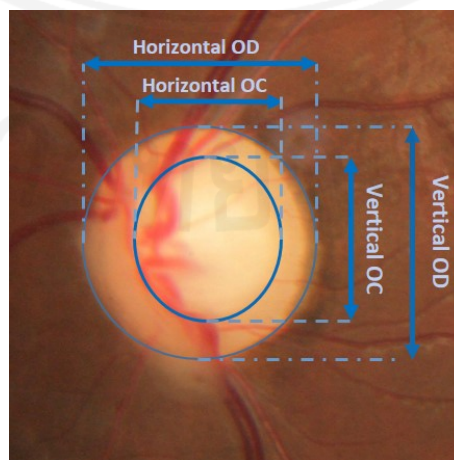
Figure 3.5: Features from CDR indicator
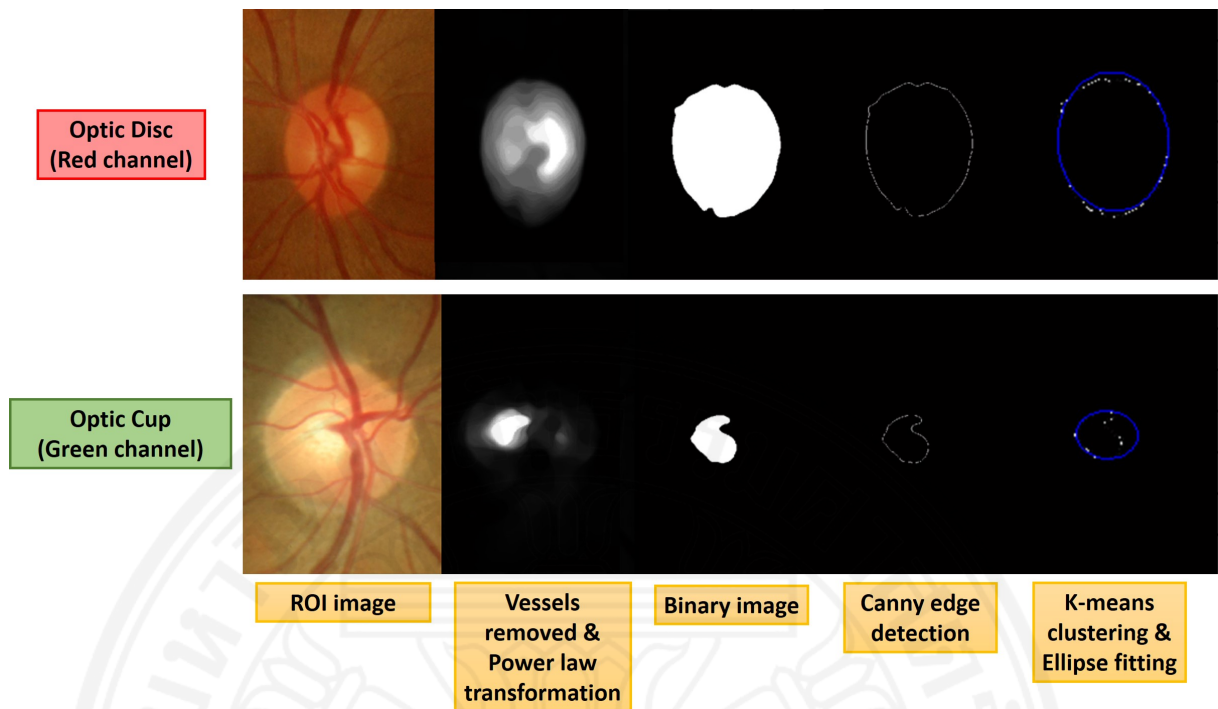
Figure 3.6: Steps of retinal analysis based on CDR indicator

3.2.2 Rim Width based on ISNT Rule

Rim width based on ISNT rule is another indicator that is used for image analysis process. As its name, the rim width of ONH is an attention point of this indicator. Hence, it can use to enhace the screening algorithm for myopia ONH and genetically large optic cup ONH. Figure 3.7 is a framework for image analysis using rim width based on ISNT rule as an indicator.

OD Segmentation

As mentioned, image analysis using rim width based on ISNT and using CDR are processed as a parallel operation. Therefore, ROI images are also input images for this analysis. OD segmentation is the first step. It consists of two sub-steps; detection of optic disc (OD) and its centroid which are shown in Figure 3.8. In this step, ROI images is read in red channel because optic disc can be clearly recognize in this color channels than others. After reading ROI images in red channel, it is called R images. Then, converting R images into binary images which white area (pixels with value '1') is an optic disc (OD) and other pixels (with value '0', black) are background. This binary images are called OD binary mages. Finding the centroid (C_x, C_y) of the optic disc (white area) from the OD binary image is an end step

Rim Width based on ISNT Rule

OD SEGMENTATION
Centroid extraction (C_x, C_y)

VESSEL TRACKING
Hessian based Filter

ISNT SEGMENTATION
ISNT Mask Generation

DETECTION
Optic Cup

FEATURE EXTRACTION
Rim Width Measurement
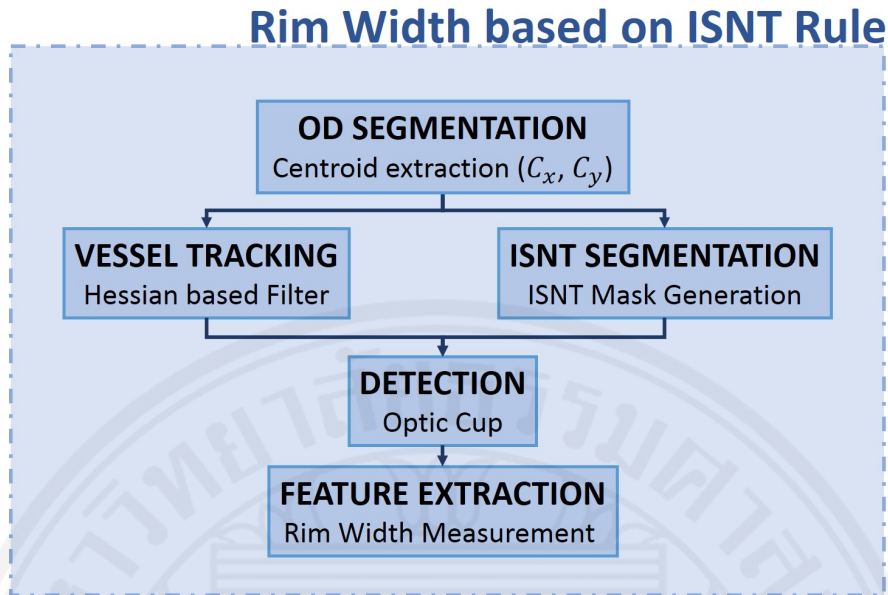
Figure 3.7: Framework of rim width based on ISNT rule

| ROI image | R image | OD Binary image | Centroid (Cx,Cy) |
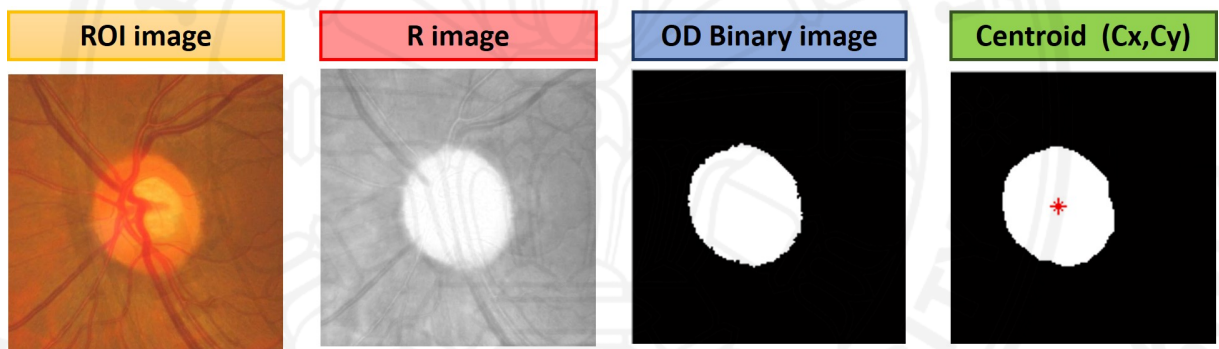
Figure 3.8: OD segmentation steps for image analysis using rim width based on ISNT rule

for the OD segmentation. Next steps are vessels tracking and ISNT segmentation which are processed in parallel.

Vessel Tracking

For vessels tracking, ROI images are read in green channel with the same reason as reading ROI images in red channel for optic disc detection. In green channel, retinal vessels are more notify than in other channels. However, before starting vessel tracking steps, ROI images should be multiply with OD binary images to remain only the OD region which is our interested in this section and also to reduce a computational cost for following steps. Vessels in a retina are vary in size, as a result, multi-scale vessel enhancement is the most suitable technique [20], [38]. Fragi filter is a multi-scale vessel enhancement which is selected to be used for this study. This filter is a Hessian-based vessel enhancement. Hessian matrix

21

$(\mathscr{H}_\sigma(I,x))$ is a second-order partial derivation which is a convolution of input image (I) at point x and Gaussian filter $\mathscr{G}_\sigma(x)$ at scale σ, as in Equation 3.5. Later, eigenvalues (λ_1, λ_2) of Hessian filter and principle direction $(\bar{u}_1, \bar{u}_2)$ are extracted from local second order structure of the image [6]. These two can be utilized to differentiate different orientation patterns of the image, blob-like structure and background structure. Using these information, vesselness function $(\mathscr{V}_F^\sigma$, Equation3.6) can be designed [2]. This function is used to distinguish blob-like and background structure. Vessels images are the output images of the vessel tracking step. An example of vessels image is shown in Figure 3.9.

$$\mathscr{H}_\sigma(I,x) = \frac{\partial^2 I_\sigma}{\partial x^2} = I(x) * \frac{\partial^2 \mathscr{G}_\sigma(x)}{\partial x^2} \tag{3.5}$$

where $\mathscr{H}_\sigma(I,x)$: is the Hessian matrix.

     $I(x)$: is a input image at point x.

     $\mathscr{G}_\sigma(x)$: is a Gaussian function with standard deviation σ.

$$\mathscr{V}_F^\sigma = exp(\frac{-\mathscr{R}_B^2}{2\beta^2})(1 - exp(-\frac{S^2}{2c^2})) \tag{3.6}$$

$$\mathscr{R}_B = \frac{|\lambda_2|}{|\lambda_1|} \tag{3.7}$$

$$S = \sqrt{\lambda_1^2 + \lambda_2^2} \tag{3.8}$$

where $\mathscr{V}_F^\sigma$: is a vesselness function.

     $\mathscr{R}_B$: is a blob-like structure (Equation 3.7).

     S : is a background structure (Equation 3.8).

     β, c : are parameters for controlling sensitivity of the filter.

     λ_1, λ_2 : are eigenvalues of Hessian matrix, $\lambda_2 > \lambda_1 > 0$.
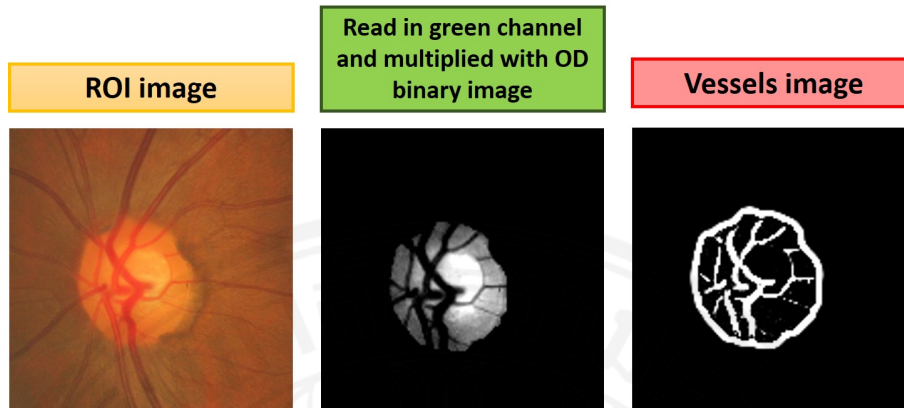
Figure 3.9: Input and output Vessel tracking steps

Even through, a second derivative filter has more noise sensitivity than a first derivative filter. However, it is better for tracking a center of vessels rather than a first derivative that suitable for tracking vessels boundaries [17]. In this study, center of the vessels is more important than the boundaries because it is necessary for finding vessels bending which will be explained in optic cup detection section.

ISNT Segmentation

While vessel tracking is processing, ISNT segmentation is also executes. In this step, ONH is separated into four regions; I, S, N, and T. The separation can be done by using ISNT masks. Knowing anatomy of ONH is needed for the mask production. ONH can be divided into four equally divisions; bottommost, uppermost, leftmost and rightmost. A bottommost region and an inferior region is the same region. A superior region is a uppermost one. While left and right region can be both nasal and temporal region because an eye-side of the ONH has not been identified. As a result, this step is generated four masks which are called Inferior mask (I), Superior mask (S), Leftmost mask (L), and Rightmost mask (R).

Rather than using only ISNT region, which is explained in Figure 3.10, as a based information for the masks production. The centroid (C_x, C_y) of ONH is also used as a reference point for generating the four masks. This centroid had been found since the OD segmentation step. Utilizing centroid as a reference point is necessary because not every ONH centroid is located at the center of the ROI images. There are three possible locations of the centroid:

- $C_x = C_y$, an ONH centroid is perfectly located at the center of a ROI image.
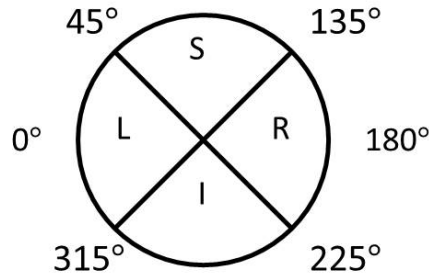
Figure 3.10: A distribution of an ONH
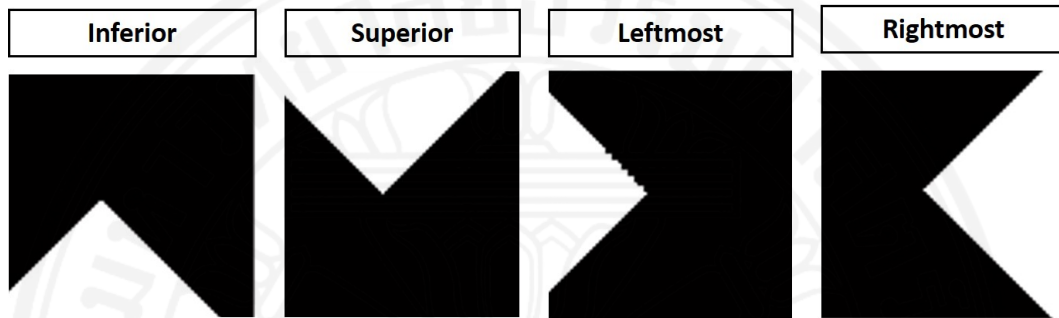
Figure 3.11: An example of four masks

- $C_x > C_y$, an ONH centroid is located at left side of a ROI image.

- $C_x < C_y$, an ONH centroid is located at the right side of a ROI image.

After gathering a region distribution with the centroid information, four masks (one set of masks) is produced. Figure 3.11 shows an example of four masks which its ONH is not located at the center of a ROI image. These masks can be used to separate one retinal image into four-sub images based on ONH region.

Detection

This step is an optic cup (OC) detection step. The optic cup is detected by using retina vessels bending which is a different technique from the optic cup detection in CDR process. At first, vessel images have to be separated into each region. To isolate a vessel image into four sub-images can be done by the following steps:

- **Step 1** : Multiply ISNT mask with the OD binary image, which is generated in OD segmentation step.

- **Step 2** : Multiply a vessel image with isolated OD binary images, which are output images from the step 1.

24
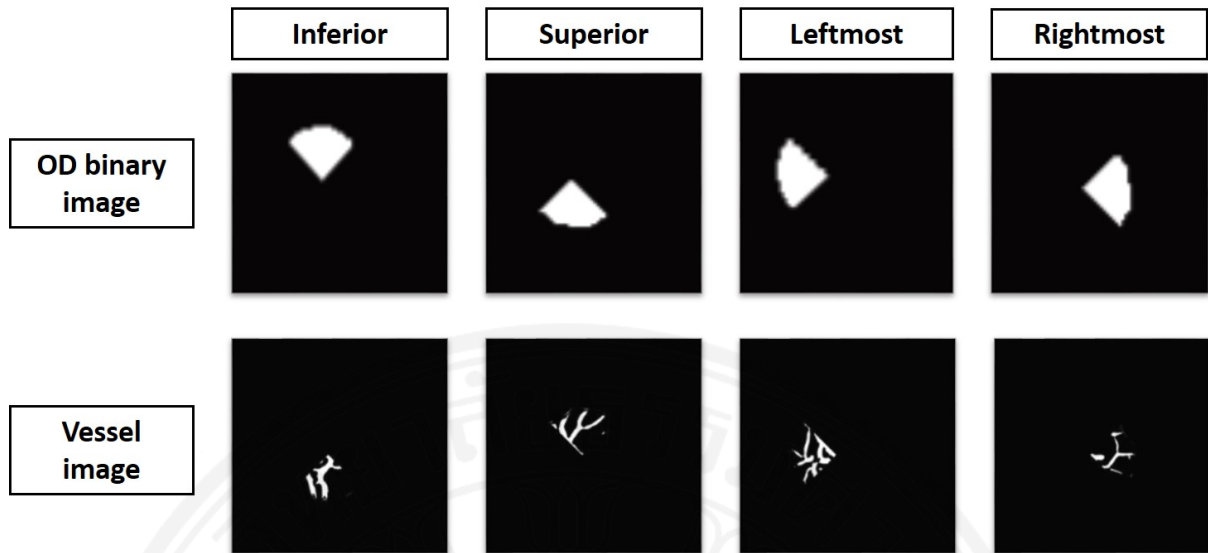
Figure 3.12: Isolated images of an OD binary images and a vessel image

The four sub-images can be called as Inferior vessel image, Superior vessel image, Leftmost vessel image, and Rightmost vessel image. The output images from both step 1 and step 2 are shown in Figure 3.12.

Then, these isolated vessel images are adopted for detecting optic cup (OC) boundaries in each region of an ONH. Beside from detecting OC boundaries, the isolated vessel images can be used to distinguish between left eyes and right eyes. As mentioned, right eyes have more vessels in right side of a ONH, whereas ONH with more vessels in left side can be indicated as left eyes. This means, comparing a leftmost vessel image with a rightmost vessel image from the same vessel image can help to classify the side of an eye. If more vessels (white pixels) are found in the leftmost vessel image, that ONH is a left eye and the image can be indicated as Nasal vessel image while Temporal vessel image is a name of the rightmost vessel image. Conversely, a right eye has more vessels in the rightmost vessel image and its Nasal vessel image is the rightmost vessel image, not the leftmost vessel image which becomes a Temporal vessel image for this case. Dissimilarity of a left eye and a right eye is exhibited in Figure 3.13.

Finding vessels centerline is a next step. Because of varies in size of retinal vessels, finding its centerline is helpful for finding its bending point. Distance transform is performed. It consists of two seeds, single-seed seeded and boundary-seed field. The shortest paths of vessels are explored by a single-seed seeded. Boundary-seed field is used to find center points between two boundaries along vessel lines. Combining these two seeds, skeleton line or a
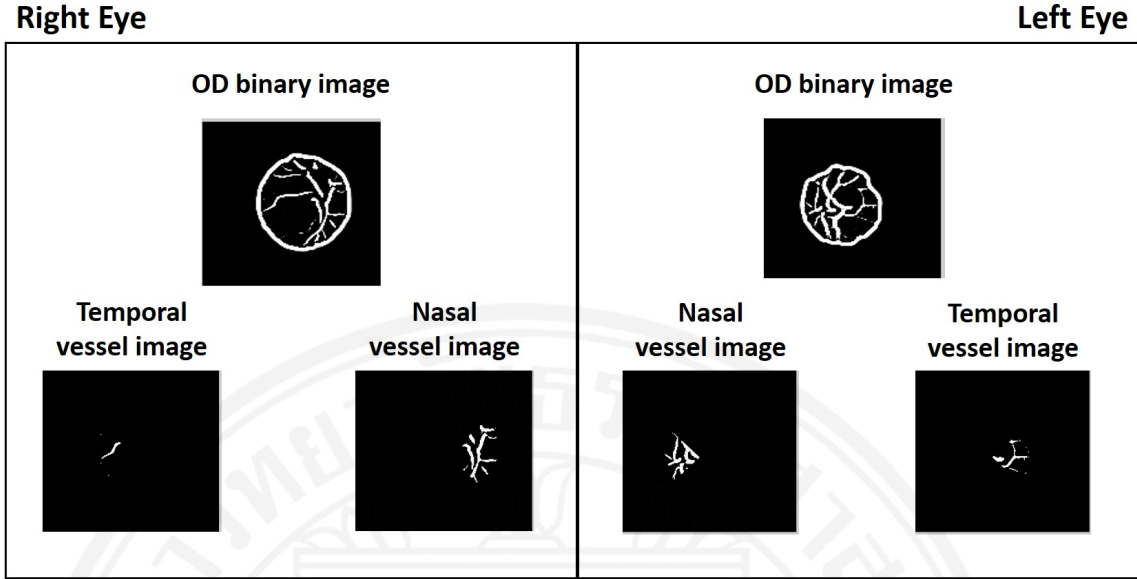
Right Eye   **Left Eye**

Figure 3.13: A differentiate between a left eye and a right eye

centerline of vessels is created.

The following step is finding vessel bending points in each region of an ONH. Isolated vessel images are used as initial images for this finding. Searching for bending candidate point is the first step. The candidate points are endpoints of vessels and junctions of vessels [38]. After all the candidates are detected, measuring bending angles of every candidate is the next step. The bending angles can be calculated by using Equation 3.9.

$$\theta = cos^{-1}\left(\frac{v_1 \cdot v_2}{|v_1||v_2|}\right) \tag{3.9}$$

where θ : is a bending angle.

     v_1, v_2 : are vectors that create the junction as shown in Figure 3.14, $\vec{AB}$ and $\vec{AC}$.

Only vessels that are bending into optic cup are interested. Therefore, junction points with the bending angle more than $170°$ are eliminated [9]. For enduring junction points, its bending angles are compared. The junction that creates the smallest bending angle in each region of an eye is chosen as a optic cup boundary for each region. Figure 3.15 shows a comparison of an optic cup boundary detection between searching by the proposed algorithm and hand-drawing from the expert.
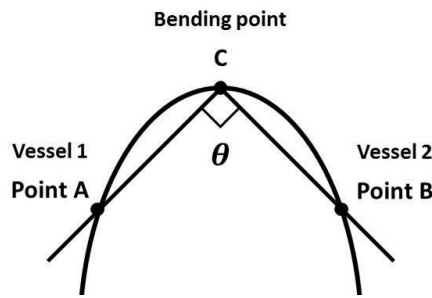
Figure 3.14: A junction point of two vessels

(a)   (b)
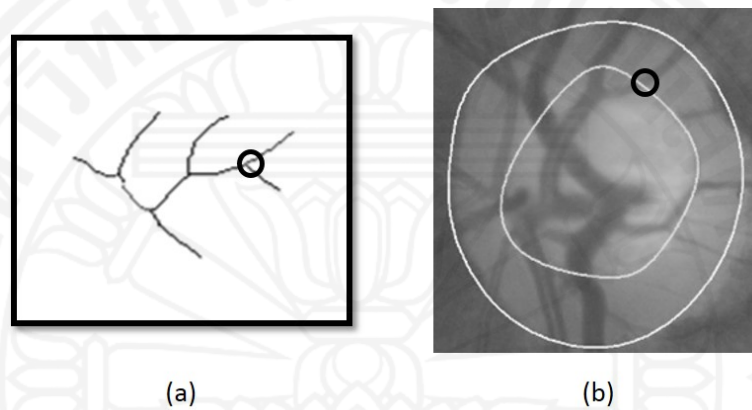
Figure 3.15: A comparison of optic cup boundary detection
(a) the proposed algorithm (b) Hand-drawing from the ophthalmologist

Feature Extraction

After optic cup boundaries of each region are identified, rim width of each region can be measured. A measurement of rim width in an ONH is displayed in Figure 3.16. The black lines are the rim width in each eye region that are used as a feature for classification, while optic cup boundary is represented by a green line. However, not every ONH has a clearly seen bending vessels in the temporal region (T). As a result, only vessels bending points in the other three regions are used as features in this study (I, S, and N). In addition rim width ratio can be another feature from this analysis process. According to ISNT rule, the rim width of non-glaucoma ONH should be arranged as the following sequence, I $>$S $>$N $>$T. Therefore if an ONH is a non-glaucoma ONH, $(\frac{I}{S}, \frac{I}{N}, and \frac{S}{N})$ should be greater than one. In the classification process, these rim width and rim width ratio are other features that are additional features besides the features from CDR analysis to classify a glaucoma status.
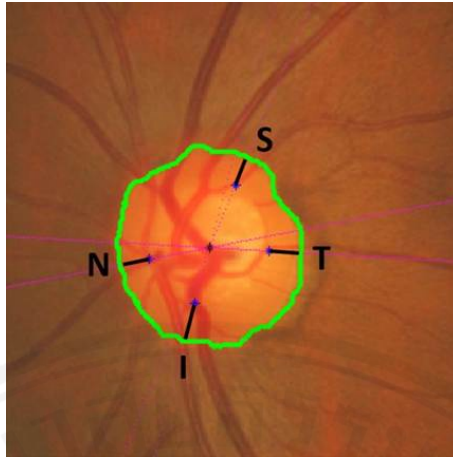
Figure 3.16: A rim width measurement

3.3 Classification

This is the last process of the proposed screening system. All information of an ONH from the image analysis process are used as features of an automatic glaucoma classifier. Four sets of feature are used in the classification:

- **Horizontal** : Diameter of an optic cup and an optic disc with CDR in horizontal direction (DOC_H, DOD_H, CDR_H) and a combination of these three features (Horizontal ALL).

- **Vertical** : Diameter of an optic cup and an optic disc with CDR in vertical direction (DOC_V, DOD_V, CDR_V) and a combination of these three features (Vertical ALL).

- **Rim Width** : Rim width in I, S, and N regions of an eye (ISNT) with rim width ratio between two region of the same ONH; $\frac{I}{S}$, $\frac{I}{N}$, and $\frac{S}{N}$ (ISNT_R) and a combination of these two features (ISNT ALL).

- **Combination** : Combination feature sets of the best feature in the other feature sets.

3.3.1 Support Vector Machine

Support vector machine with linear kernel function is an automatic binary classifier for this system. The input data are isolated into two classes by assign a target to be 0 for glaucoma cases and 1 for non-glaucoma cases. Then, examining them by the generated classifier using a 10-fold cross validation technique. Firstly, the data set is randomly separated into two sets. The first set is a testing set which is 10 percent of the data set. The remaining data, another

90 percent of the data, are set as a training set. All data are processed by the classifier based on input features. These steps are repeated for10 times. Afterwards, all data are classified.

Chapter 4

Results and Analysis

The performance of screening algorithms for glaucoma are demonstrated in this chapter. The first screening algorithm is using only extracted features from cup-to-disc ratio indicator. The other two feature sets for the second algorithm is extracted from an indicator called Rim width based on ISNT rule. Combination of features from both cup-to-disc ratio and rim width based on ISNT rule are proposed in the last screening algorithm which is our proposed screening algorithm. Additionally, the results from every features are analyzed by compare them with clinical results.

4.1 Clinical Results

As mentioned, the clinical results are obtained from Mettapracharak hospital. The data set is analyzed by using cup-to-disc ratio indicator. An eye with CDR value greater than 0.65 is classified as glaucoma eye. Otherwise, it is a non-glaucoma ONH.

4.2 Evaluation

The confusion matrix is performed to evaluate the performance of each input feature for the SVM comparing to the clinical results. Six indicators are defined in a confusion matrix; True positive (TP), True negative (TF), False positive (FP), False negative (FN), Accuracy (ACC.), Specificity (SPEC.), and Sensitivity (SENS.).

The true positive value represents cases that is correctly indicated as glaucoma while the correctness of non-glaucoma indication is represented by the true negative value. The incorrectly indication as glaucoma and non-glaucoma which are important indicators for this study are represented by false positive and false negative value. Accuracy, specificity, and sensitivity are correctness of overall performance, non-glaucoma indication, and glaucoma indication in term of percentage. These three indicators can be calculated by using Equation 4.1 - 4.3.

$$ACC = \frac{TP + TN}{TP + TN + FP + FN} \qquad (4.1)$$

30

$$SPEC = \frac{TN}{TN+FP} \qquad (4.2)$$

$$SENS = \frac{TP}{TP+FN} \qquad (4.3)$$

4.3 Cup-to-disc Ratio Features

Even through ophthalmologists are concerned about a vertical cup-to-disc ratio (CDR_V) which are calculated by using vertical diameter of an optic cup (DOC_V) and an optic disc (DOD_V). All the three data and a combination of these three data (Vertical ALL) are used as features to classify glaucoma status. To improve a performance of the screening algorithm, horizontal cup-to-disc ratio (CDR_H), horizontal optic cup diameter (DOC_H), horizontal optic disc diameter (DOD_H), and a combination of all horizontal data (Horizontal ALL) are also included as the other features for the screening algorithm. Therefore, the total of eight features are utilized with the SVM for the classification. Summarize results for each feature are shown in Table 4.1 - 4.4 and Table 4.6 - 4.9 according to the following order: DOC_H, DOD_H, CDR_H, Horizontal ALL, DOC_V, DOD_V, CDR_V, and Vertical ALL. Table 4.5 and 4.10 display a comparison result among features in the horizontal set and the vertical set, respectively.

Table 4.1: Confusion matrix of the horizontal DOC feature

	Clinical		
	Glaucoma	Non-Glaucoma	
TP	**FP**	**PREC.**
37	**14**	**72.5%**
32.7%	12.4%	27.5%
FN	**TN**	**NPV.**
17	**45**	**72.6%**
15.0%	39.8%	27.4%
SENS.	**SPEC.**	**ACC.**
68.5%	**76.3%**	**72.6%**
31.5%	23.7%	27.4%

Table 4.2: Confusion matrix of the horizontal DOD feature

	Clinical		
	Glaucoma	Non-Glaucoma	
Glaucoma (Horizontal DOD (DOD_H))	**TP** 19 16.8%	**FP** 18 15.9%	**PREC.** 51.4% 48.6%
Non-Glaucoma	**FN** 35 31.0%	**TN** 41 36.3%	**NPV.** 53.9% 46.1%
	SENS. 35.2% 64.8%	**SPEC.** 69.5% 30.5%	**ACC.** 53.1% 46.9%

Table 4.3: Confusion matrix of the horizontal CDR feature

	Clinical		
	Glaucoma	Non-Glaucoma	
Glaucoma (Horizontal CDR (CDR_H))	**TP** 41 36.3%	**FP** 13 11.5%	**PREC.** 75.9% 24.1%
Non-Glaucoma	**FN** 13 11.5%	**TN** 46 40.7%	**NPV.** 78.0% 22.0%
	SENS. 75.9% 24.1%	**SPEC.** 78.0% 22.0%	**ACC.** 77.0% 23.0%

Table 4.4: Confusion matrix of the combination of all horizontal features

Clinical

	Glaucoma	Non-Glaucoma	
Glaucoma	TP **38** 33.6%	FP **11** 9.7%	PREC. **77.6%** 22.4%
Non-Glaucoma	FN **16** 14.2%	TN **48** 42.5%	NPV. **75.0%** 25.0%
	SENS. **70.4%** 29.6%	SPEC. **81.4%** 18.6%	ACC. **76.1%** 23.9%

Horizontal ALL (DOD_H, DOC_H, CDR_H)

Table 4.5: Comparison among four features of horizontal set feature

	Horizontal Cup Model	Horizontal Disc Model	Horizontal CDR Model	Horizontal ALL
TP	37	19	*41*	38
TN	45	41	*46*	48
FP	14	18	*13*	11
FN	17	35	*13*	16
ACC.	72.6%	53.1%	*77.0%*	76.1%
SPEC.	76.3%	69.5%	*78.0%*	81.4%
SENS.	68.5%	35.2%	*75.9%*	70.4%

Table 4.6: Confusion matrix of the vertical DOC feature

	Clinical		
	Glaucoma	Non-Glaucoma	
Glaucoma	TP 40 35.4%	FP 14 12.4%	PREC. 74.1% 25.9%
Non-Glaucoma	FN 14 12.4%	TN 45 39.8%	NPV. 76.3% 23.7%
	SENS. 74.1% 25.9%	SPEC. 76.3% 23.7%	ACC. 75.2% 24.8%

Vertical DOC (DOC_V)

Table 4.7: Confusion matrix of the vertical DOD feature

	Clinical		
	Glaucoma	Non-Glaucoma	
Glaucoma	TP 15 13.3%	FP 12 10.6%	PREC. 55.6% 44.4%
Non-Glaucoma	FN 39 34.5%	TN 47 41.6%	NPV. 54.7% 45.3%
	SENS. 27.8% 72.2%	SPEC. 79.7% 20.3%	ACC. 54.9% 45.1%

Vertical DOD (DOD_V)

Table 4.8: Confusion matrix of the vertical CDR feature

	Clinical		
	Glaucoma	Non-Glaucoma	
TP **46** 40.7%	**FP** **12** 10.6%	**PREC.** **79.3%** 20.7%
FN **8** 7.1%	**TN** **47** 41.6%	**NPV.** **85.5%** 14.5%
SENS. **85.2%** 14.8%	**SPEC.** **79.7%** 20.3%	**ACC.** **82.3%** 17.7%

Vertical CDR (CDR_V) — Glaucoma / Non-Glaucoma

Table 4.9: Confusion matrix of the combination of all vertical features

	Clinical		
	Glaucoma	Non-Glaucoma	
TP **44** 38.9%	**FP** **12** 10.6%	**PREC.** **78.6%** 21.4%
FN **10** 8.8%	**TN** **47** 41.6%	**NPV.** **82.5%** 17.5%
SENS. **81.5%** 18.5%	**SPEC.** **79.7%** 20.3%	**ACC.** **80.5%** 19.5%

Vertical ALL (DOD_V, DOC_V, CDR_V) — Glaucoma / Non-Glaucoma

35

Table 4.10: Comparison among four features of a Vertical set feature

	Vertical Cup Model	Vertical Disc Model	Vertical CDR Model	Vertical ALL
TP	40	15	*46*	44
TN	45	47	*47*	47
FP	14	12	*12*	12
FN	14	39	*8*	10
ACC.	75.2%	54.9%	*82.3%*	80.5%
SPEC.	76.3%	79.7%	*79.7%*	79.7%
SENS.	74.1%	27.8%	*85.2%*	81.5%

4.4 Rim Width based on ISNT Rule Features

The same data is tested by the SVM with different features. The feature sets which based on ISNT rule are used as the input features in this part. Table 4.11 - 4.13 are summarized tables for ISNT rim width (ISNT), ISNT ratio (ISNT_R) and a combination of the two features (ISNT_ALL), respectively. A comparison table among the results from each features are shown in Table 4.14.

Table 4.11: Confusion matrix of the ISNT rim width feature

		Clinical		
		Glaucoma	Non-Glaucoma	
ISNT Rim Width (ISNT)	Glaucoma	**TP** 44 38.9%	**FP** 4 3.5%	**PREC.** 91.7% 8.3%
	Non-Glaucoma	**FN** 10 8.8%	**TN** 55 48.7%	**NPV.** 84.6% 15.4%
		SENS. 81.5% 18.5%	**SPEC.** 93.2% 6.8%	**ACC.** 87.6% 12.4%

Table 4.12: Confusion matrix of the ISNT ratio feature

| | | Clinical | | |
		Glaucoma	Non-Glaucoma	
ISNT Ratio (ISNT_R)	Glaucoma	**TP** **48** 42.5%	**FP** **4** 3.5%	**PREC.** **92.3%** 7.7%
	Non-Glaucoma	**FN** **6** 5.3%	**TN** **55** 48.7%	**NPV.** **90.2%** 9.8%
		SENS. **88.9%** 11.1%	**SPEC.** **93.2%** 6.8%	**ACC.** **91.2%** 8.8%

Table 4.13: Confusion matrix of the combination of all ISNT features

| | | Clinical | | |
		Glaucoma	Non-Glaucoma	
ISNT ALL (ISNT, ISNT_R)	Glaucoma	**TP** **48** 42.5%	**FP** **4** 3.5%	**PREC.** **92.3%** 7.7%
	Non-Glaucoma	**FN** **6** 5.3%	**TN** **55** 48.7%	**NPV.** **90.2%** 9.8%
		SENS. **88.9%** 11.1%	**SPEC.** **93.2%** 6.8%	**ACC.** **91.2%** 8.8%

Table 4.14: Comparison among three features of a Rim width set feature

	ISNT Rim Width Model	ISNT Ratio Model	ISNT ALL
TP	44	*48*	48
TN	55	*55*	55
FP	4	*4*	4
FN	10	*6*	6
ACC.	87.6%	*91.2%*	91.2%
SPEC.	93.2%	*93.2%*	93.2%
SENS.	81.5%	*88.9%*	88.9%

4.5 Proposed Features

The proposed features are an integration of the best feature from each feature set; a horizontal set, a vertical set, and a rim width set. According to Table 4.5 and 4.10, using only and horizontal CDR (CDR_H) and vertical CDR (CDR_V) as an input feature give the most accuracy among the features in the horizontal set and the vertical set feature, respectively. Therefore, these two features are selected to be used in our proposed feature. For the Rim width feature set, both ISNT_R model and ISNT ALL model give the same accuracy. However, ISNT_R model is selected because of its less computational time according to its less input data for the SVM. From the selected features, four combination features are created. Two features from the selected feature are combined to create the first three features; CDR_V and CDR_H model, CDR_V and ISNT_R model, and CDR_H and ISNT_R model . The last model or the proposed model is used CDR_H together with CDR_V and ISNT_R as input features for the SVM. Results from the four combination models are shown in Table 4.15 - 4.18 in the same order as the description. The performances of each combination model are compared in Table 4.14.

According to the performance of each feature sets in Table 4.5, 4.10, 4.14, and 4.19, the combination feature set give the best performance among all. By observing among all input features of the combination feature set, the CDR_V and ISNT_R model give the most accuracy value (93.8%). Meanwhile, the least accuracy model is a CDR_H and CDR_V model (83.2%). False positive and false negative are the other values that we concern because it may result in an insufficient classification. By comparing false positive and false negative

value of all model, the CDR_V and ISNT_R model has the smallest number of FP case which is 3 cases while the proposed model (CDR_V with CDR_H and ISNT_R) give only 1 FN case which is the smallest value among all models. Although the CDR_V and ISNT_R model give the most accuracy performance and the smallest value of false positive case. However, false negative case is a more serious error. The reason is false negative case means a glaucoma case is incorrectly classified as a non-glaucomal case. This may result in a late treatment and the eye becomes more illness. Therefore, the purposed model is indicated as the best model among all according to the least FN case and its accuracy (92.9%) is just 0.9% less than the CDR_V and ISNT_R model.

Table 4.15: Confusion matrix of the combination of CDR_V and CDR_H feature

		Clinical		
		Glaucoma	Non-Glaucoma	
CDR_V & CDR_H	Glaucoma	TP 47 41.6%	FP 12 10.6%	PREC. 79.7% 20.3%
	Non-Glaucoma	FN 7 6.2%	TN 47 41.6%	NPV. 87.0% 13.0%
		SENS. 87.0% 13.0%	SPEC. 79.7% 20.3%	ACC. 83.2% 16.8%

Table 4.16: Confusion matrix of the combination of CDR_V and ISNT_R feature

	Clinical		
	Glaucoma	Non-Glaucoma	
TP 51 45.1%	**FP** 4 3.5%	**PREC.** 92.7% 7.3%
FN 3 2.7%	**TN** 55 48.7%	**NPV.** 94.8% 5.2%
SENS. 94.4% 5.6%	**SPEC.** 93.2% 6.8%	**ACC.** 93.8% 6.2%

Table 4.17: Confusion matrix of the combination of CDR_H and ISNT_R feature

	Clinical		
	Glaucoma	Non-Glaucoma	
TP 48 42.5%	**FP** 6 5.3%	**PREC.** 88.9% 11.1%
FN 6 5.3%	**TN** 53 46.9%	**NPV.** 89.8% 10.2%
SENS. 88.9% 11.1%	**SPEC.** 89.8% 10.2%	**ACC.** 89.4% 10.6%

Table 4.18: Confusion matrix of the combination of CDR_V, CDR_H, and ISNT_R feature

	Clinical		
	Glaucoma	Non-Glaucoma	
Glaucoma	TP 53 46.9%	FP 7 6.2%	PREC. 88.3% 11.7%
Non-Glaucoma	FN 1 0.9%	TN 52 46.0%	NPV. 98.1% 1.9%
	SENS. 98.1% 1.9%	SPEC. 88.1% 11.9%	ACC. 92.9% 7.1%

Table 4.19: Comparison among all three features of a Combination set feature

	CDR_V & CDR_H Model	CDR_V & ISNT_R Model	CDR_H & ISNT_R Model	CDR_V & CDR_H & ISNT_R Model
TP	47	51	48	53
TN	47	55	53	52
FP	12	4	6	7
FN	7	3	6	1
ACC.	83.2%	93.8%	89.4%	92.9%
SPEC.	79.7%	93.2%	89.8%	88.1%
SENS.	87.0%	94.4%	88.9%	98.1%

Chapter 5

Conclusion

Nowadays, glaucoma analysis can be done by expert ophthalmologists at hospitals. However, a lack of equipment and ophthalmologists which are important for glaucoma analysis are the main problems. The main purpose of this study is to overcome these limitations by developing an automatic glaucoma screening algorithm which has inexpensive cost and can be used by untrained ophthalmologists. Retina fundus images are utilized as initial images for the proposed algorithm because of its inexpensiveness. Furthermore, it is an easy accessible source which can be found in every hospital. Another purpose of this study is the screening algorithm can be used for both normal eyesight and myopia (near-eyesight) eyes. The difference between a normal eyesight ONH and a myopia ONH is the size of an optic cup. Myopia ONH usually has a larger optic cup compares to other ONH.

The retinal images are processed by using image processing techniques based on two clinical indicators, cup-to-disc ratio (CDR) and rim width based on ISNT rule. CDR is the most famous indicator for glaucoma screening system which interests in the size of an optic cup. However, myopia ONH can be incorrectly classified by using only this indicator because of its optic cup. Therefore, rim width based on ISNT rule is selected to be another indicator for this screening algorithm. The large size of an optic cup cannot affect the performance of this indicator because its interested region is a rim width in each region of an ONH.

From CDR indicator, a diameter of an optic cup and an optic disc in both horizontal and vertical direction are applied in the algorithm. Rim width in inferior, superior and nasal regions and its ratio are other features that are extracted from a rim width based on ISNT rule indicator. All features are tested as input features for support vector machine which is an automatic classifier for this study. The experiment results shows that the proposed algorithm, using CDR_H together with CDR_V and ISNT_R as an input feature, is appropriated for being used with normal-eyesight and myopia eyes.

For future study, more retinal images should be tested with the proposed algorithm. Also, more indicators could be added to the algorithm for a reduction of error cases; false positive and false negative cases. Two examples of glaucoma indicators that can be extracted from retinal fundus images are presented in this section. The first indicator is asymmetry of the

optic nerve cupping between two eyes. This indicator can be used when patients has only one glaucoma eye. By comparing both eyes in term of the cup-to-disc ratio, a difference between a non-glaucoma eye and a glaucoma eye can be noticed. The second indicator is a presence of splinter hemorrhages or vessels that moving away from the rim margin. It is rarely found in non-glaucoma ONH and can be easily overlooked by human. Superotemporal and inferotemporal are the two region that it commonly occurs. Adding more features apart from indicators to an automatic classifier may help to reduce error cases. For example, dividing patients into groups based on their age and sex because different age and sex may have different standard for the classification.

Furthermore, creating the GUI for this screening system is also important. It will become a user friendly interface that is easy to be used and understand. Moreover, retina fundus images can be used for diabetes retinopathy screening. Our glaucoma screening algorithm can be merged with diabetes retinopathy screening algorithm to create an eye abnormality screening system.

References

[1] T. Kanungo, D. M. Mount, N. Netanyahu, C. Piatko, R. Silverman, and A. Y. Wu. An efficient k-means clustering algorithm: Analysis and implementation. *Proceeding IEEE Conference Computer Vision and Pattern Recognition*, pages 881–892, 2002.

[2] A. Frangi, W. Niessen, K. Vincken, and M. Viergever. Multiscale vessel enhancement filtering. *Medical Image Computing and Computer-Assisted Intervention - MICCAI98*, pages 130–137, 1998.

[3] Angele Vision Clinic. What is glaucoma? primary open angle glaucoma & narrow angle glaucoma. `http://avclinic.com/eye-conditions/glaucoma/`, 2014. Accessed on 1-July-2015.

[4] C. Burana-Anusorn, W. Kongprawechnon, T. Kondo, S. Sintuwong and K. Tungpimolrut. Image processing techniques for glaucoma detection using the cup-to-disc ratio. *Thammasat International Journal of Science and Technology*, pages 22–34, January - March 2013.

[5] Chih-Yin Ho, Tun-Wen Pai, Hao-Teng Chang ,and Hsin-Yi Chen. An automatic fundus image analysis system for clinical diagnosis of glaucoma. *International Conference on Complex, Intelligent and Software Intensive Systems*, pages 559–564, 2011.

[6] D. Jimenez-Carretero, A. Santos, S. Kerkstra, R. D. Rudyanto, and M. J. Ledesma-Carbayo. 3d frangi-based lung vessel enhancement filter penalizing airways. *IEEE 10th International Symposium on Biomedical Imaging: From Nano to Macro*, pages 926–929, April 2013.

[7] D. Yadav, M. P. Sarathi, and M. K. Dutta. Classification of glaucoma based on texture features using neural networks. *Seventh International Conference on Contemporary Computing*, pages 109–112, 2014.

[8] Darsana S. and R. M. Nair. Mask image generation for segmenting retinal fundus image features into isnt quadrants using array centroid method. *International Journal of Research in Engineering and Technology*, pages 263–267, April 2014.

[9] G. D. Joshi, J. Sivaswamy, K. Karan, Prashanth R., and S. R. Krishnadas. Vessel bend-based cup segmentation in retinal images. *IEEE International Conference on Pattern Recognition*, pages 2536–2539, 2010.

[10] G. Gupta. Algorithm for image processing using improved median filter and comparison of mean, median and improved median filter. *International Journal of Soft Computing and Engineering (IJSCE)*, pages 304–311, November 2011.

[11] Glaucoma Research Foundation. Understanding glaucoma. *Gleams*, May 2010.

[12] Glaucoma Research Foundation. Eye anatomy. *Understanding and Living with Glaucoma*, September 2013.

[13] HD Image Garelly. Fundus photograph camera. `http://cdn.lipstiq.com/wp-content/uploads/2010/10/fundus-camera.jpg`. Accessed on 2-July-2015.

[14] J. Yu, S. S. R. Abidi, P. H. Artes, A. MaIntyre, M. Heywood. Automated optic nerve analysis for diagnosis support in glaucoma. *IEEE Computer-based Medical Systems*, 2005.

[15] James B Soque. Introduction to the fluorescein angiography procedure. `http://c.ymcdn.com/sites/www.opsweb.org/resource/collection/6F6C794C-4E24-4D19-862B-9B4A8ACB70B8/FR-1-D,_Soque,__Crash_Course-_FA_section.pdf`. Accessed on 7-July-2015.

[16] K. Chan, T. Lee, P. A. Sample, M. A. Gladbaum, R. N. Weinreb, and T. J. Sejnowski. Comparison of machine learning and traditional classifiers in glaucoma diagnosis. *proceeding of IEEE Tran. on biomed. eng.*, 2012.

[17] K. Krissian, J. Ellsmere ,K. Vosburgh , R. Kikinis , and C.-F. Westin. Multiscale segmentation of the aorta in 3d ultrasound images. *Proceedings of the 25th Annual International Conference of the IEEE Engineering in Medicine and Biology Society*, pages 638–641, September 2003.

[18] K. Narasimhan, K. Vijayarekha, K.A. JogiNarayana, P. SivaPrasad and V. SatishKumar. Glaucoma detection from fundus image using opencv. *Research Journal*

of Applied Sciences, Engineering and Technology, pages 5459–5463, December 2012.

[19] L. Wang, V. Kallem, M. Bansal, J. Eledath, H. Sawhney, D. J. Pearson, and R. A. Ston. Automatic 3d change detection for glaucoma diagnosis. *IEEE Winter Conference on Applications of Computer Vision*, pages 401–408, 2014.

[20] M. H. Tan, Y. Sun, S. H. Ong, J. Liu, M. Baskaran, T. Aung and T. Y. Wong. Automatic notch detection in retinal images. *IEEE International Symposiumon Biomedical Imaging*, April 2013.

[21] Mayo Clinic Staff. Glaucoma: Symptoms. `http://www.mayoclinic.org/diseases-conditions/glaucoma/basics/symptoms/con-20024042`, October 2012. Accessed on 11-July-2015.

[22] Murray Fingeret. Cup-to-disc ratio not crucial to glaucoma documentation. `http://m1.wyanokecdn.com/392e850034823ebf40d6ab2946d5f7ef.jpg`, June 2005. Accessed on 1-July-2015.

[23] N. Efford. *Digital Image Processing: A Practical Introduction Using Java*, chapter Morphological image processing. Pearson Education, 2000.

[24] N. Harizman, C. Oliveira, A. Chiang, C. Tello, M. Marmor, R. Ritch, and J. M. Liebmann. The isnt rule and differentiation of normal from glaucomatous eyes. *Arch Ophthalmol*, pages 1579–1583, November 2006.

[25] Narit Kitnarong. Glaucoma. `http://www.si.mahidol.ac.th/Th/department/ophthalmology/dept_article_detail.asp?a_id=874`, May 2011. Accessed on 11-July-2015.

[26] National Eye Institute (NEI). Facts about glaucoma. `http://www.nei.nih.gov/health/glaucoma`, 2010. Accessed on 1-July-2015.

[27] P. Vejjanugraha, W. Kongprawechnon, T. Kondo, S. Sintuwong, and K. Tungpimolrut. An automatic glaucoma detection method using support vector machine. *SICE Annual Conference*, September 2014.

[28] R. Maini and H. Aggarwal. Study and comparison of various image edge detection techniques. *International Journal of Image Processing (IJIP)*, pages 1–11, Fabruary 2009.

[29] S. Bhartiya, R. Gadia, H. S. Sethi, and A. Panda. Clinical evaluation of optic nerve head in glaucoma. *Journal of Current Glaucoma Practice*, pages 115–132, September-December 2010.

[30] S. P. Vimal and P. K. Thiruvikraman. Automated image enhancement using power law transformations. *Sādhanā*, pages 739–745, December 2012.

[31] S. S. Lee, M. Rajeswari, D. Ramachandram, and B. Shaharuddina. Screening of diabetic retinopathy - automatic segmentation of optic disc in colour images. *The 2nd International Conference on Distributed Frameworks for Multimedia Applications*, pages 1–7, May 2006.

[32] Space healthcare. Understandung glaucoma. `http://space-healthcare.com/wp-content/uploads/2015/02/glaucoma-300x197.jpg`, 2015. Accessed on 1-July-2015.

[33] T. Root. *OphthoBook*, chapter Glaucoma, pages 33–46. Self-published. Printed by CreateSpace, 2009.

[34] Thai Eye Center. Glaucoma. `http://www.thaieye.com/glaucoma`, 2012. Accessed on 1-July-2015.

[35] The Hong Kong Medical Association. Primary open angle glaucoma. `http://www.hkma.org/english/cme/onlinecme/200809-fig1.jpg`, September 2008. Accessed on 1-July-2015.

[36] The tgf Glaucoma Foundation. Treating glaucoma. `https://www.glaucomafoundation.org/treating_glaucoma.htm`. Accessed on 11-July-2015.

[37] W. Ruengkitpinyo, W. Kongprawechnon, and T. Kondo. An image segmentation method for glaucoma detection using the cdr. *The Second Asian Conference on Information Systems (ACIS)*, November 2013.

[38] W. W. K. Damon, J. Liu, T. N. Meng, Y. Fengshou and W. T. Yin. Automatic detection of the optic cup using vessel kinking in digital retinal fundus images. *IEEE International Symposium on Biomedical Imaging (ISBI)*, pages 1647–1650, May 2012.

[39] Wang, M.Y., Maurer, C.R., Jr., Fitzpatrick, J.M. and Maciunas, R.J. An automatic technique forfinding and localizing externally attached markers in ct and mr volume images of the head. *IEEE Transactions on Biomedical Engineering*, pages 627–637, August 2002.

[40] WhittenLaserEye. Eye anatomy. `http://www.whittenlasereye.com/images/eye-anatomy.gif`. Accessed on 7-July-2015.